Corrosion and Corrosion Inhibition of Pure Iron in Neutral Chloride Solutions by 1,1'-Thiocarbonyldiimidazole

El-Sayed M. Sherif [1,*]

[1] Center of Excellence for Research in Engineering Materials (CEREM), College of Engineering, King Saud University, P. O. Box 800, Al-Riyadh 11421, Saudi Arabia

[*]E-mail: esherif@ksu.edu.sa

The corrosion behavior of pure iron in naturally aerated stagnant solutions of 3.5% NaCl and its inhibition by 1,1'-thiocarbonyldiimidazole have been reported. The study was carried out using open-circuit potential, cyclic potentiodynamic polarization, potentiostatic current-time, and electrochemical impedance spectroscopy measurements. The corroded and inhibited iron surfaces were characterized by in-situ Raman spectroscopy, scanning electron microscopy and energy dispersive X-ray investigations. Results obtained revealed that the addition of the inhibitor decreased the pitting and uniform corrosion reactions of iron in aerated 3.5% NaCl solutions. This effect was found to increase by increasing the concentration of the inhibitor from 0.5 mM to 2.0 mM due to the adsorption of its molecules onto iron preventing the formation of ferrous and ferric chlorides and blocking flawed areas on the electrode surface. The adsorption of the inhibitor molecules onto the iron surface was confirmed by scanning electron microscope, energy dispersive X-ray and in-situ Raman spectroscopy investigations.

1. INTRODUCTION

Iron has been one of the most widely used materials in our daily life for its unlimited applications. The corrosion and corrosion protection of iron in corrosive environments have attracted the attention of many investigators [1-4]. One of the most important methods in the protection of metals against corrosion is the use of organic inhibitors [5-9]. Organic compounds containing nitrogen, sulfur or oxygen atoms and aromatic rings or multiple bonds in their molecular structure have been reported to be good inhibitors to mitigate the corrosion of metals in corrosive media [10, 11]. The

effectiveness of these corrosion inhibitors mainly depends on the physicochemical and electronic properties of the organic compound molecule which in turn are related to its functional groups, steric effects, electronic density of donor atoms, and p-orbital character of donating electrons [12, 13]. It has been also reported [1, 2, 13] that efficient inhibitors should chemisorb on the metal surface, be polymeric or polymerize in-situ on the metal, form a defect free, compact barrier film that increases the inner layer thickness and finally have high adsorption energy on the metal surface.

There is a growing trend to study environment friendly inhibitors recently [14, 15]. It has been reported that non-toxic imidazole and its derivatives are well-known corrosion inhibitors for metals and alloys [16]. Imidazoles are organic compounds with two nitrogen atoms in the heterocyclic ring. The imidazole molecule shows three different possible anchoring sites suitable for bonding; these are pyridine like nitrogen atom 3 N, pyrrole like nitrogen atom 1 N and aromatic ring itself and probably the substituent may act as an active center [15, 17]. The inhibition mechanism usually invokes their interactions with the metallic surfaces via their adsorption sites where polar functional groups are usually regarded as the reaction centers [9]. Lukovits et al. [18] have also reported that the inhibitor molecules are bonded to the metal surface by chemisorption, physisorption, or complexation with the polar groups acting as the reactive centers in the molecules.

The purpose of this work is to investigate the corrosion reactions of pure iron in 3.5% sodium chloride solutions and inhibiting these reactions by 1,1'-thiocarbonyldiimidazole (TCDI), whose effects on iron corrosion in aggressive media have not been reported previously. The chemical formula of TCDI is shown in Fig. 1.
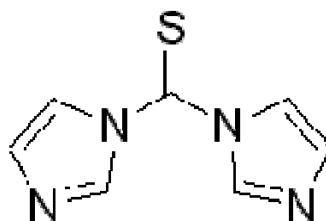
Figure 1. Chemical formula of 1,1'-thiocarbonyldiimidazole (TCDI).

In order to achieve this purpose, the study was carried out using electrochemical techniques such as open circuit potential, cyclic potentiodynamic polarization, potentiostatic current-time, and electrochemical impedance spectroscopy measurements. The work was also complemented by scanning electron microscopy (SEM), energy dispersive X-ray (EDX), and in-situ Raman spectroscopy investigations. The SEM and EDX were employed to examine the surface morphology as well as to determine the elements of TCDI on the iron surface. While, the in-situ Raman spectroscopy experiments we performed to reveal the inhibition of iron corrosion by TCDI at the molecular level.

2. EXPERIMENTAL PROCEDURE

2.1. Chemicals and electrochemical cell

1,1'-thiocarbonyldiimidazole (TCDI, Alfa-Aesar, 94%), sodium chloride (NaCl, Merck, 99%), and absolute ethanol (C_2H_5OH, Merck, 99.9%) were used as received. An electrochemical cell with a three-electrode configuration was used for electrochemical measurements; a pure iron rod (Fe, 99.98%, 9.5 mm in diameter), a platinum foil, and a Metrohm Ag/AgCl electrode (in 3 M KCl) were used as a working, counter, and reference electrodes, respectively. The iron electrode was first polished successively with metallographic emery paper of increasing fineness of up to 800 grits, and then further with 5, 1, 0.5 and 0.3 µm alumina slurries (Buehler). The electrode was then washed with doubly distilled water, degreased with acetone, washed using doubly distilled water again and finally dried with tissue paper.

2.2. Electrochemical methods

Electrochemical experiments were performed by using a PARC Parstat-2273 Advanced Electrochemical System after immersing the iron electrode for 1h in 3.5% NaCl solution in the absence and presence of 0.50, 1.0, and 2.0 mM TCDI present. Only the open-circuit potential (OCP) curves were recorded from the first moment of iron immersion in freely aerated test solution without and with TCDI by continuously measuring the change of the potential for 12 h. The cyclic potentiodynamic polarization curves were obtained by scanning the potential of iron from -1200 to 250 mV at a scan rate of 1 mV/s. Potentiostatic current-time experiments were carried out by stepping a constant potential value of -500 mV for 120 min. Electrochemical impedance spectroscopy (EIS) tests were performed at corrosion potentials (E_{Corr}) over a frequency range of 100 kHz − 0.1 Hz, with an ac wave of ±5 mV peak-to-peak overlaid on a dc bias potential, and the impedance data were collected using Powersine software at a rate of 10 points per decade change in frequency. All measurements were carried out at room temperature.

2.3. In-situ Raman spectroscopy

The in-situ Raman spectroscopy investigations in this study were obtained as reported in the previous work [1]. In brief, a special made Teflon cell was used for the in-situ Raman investigations. The working electrode was a 9.5 mm diameter iron surface, which was polished and cleaned as for cases of iron rods. The surface of this working electrode was positioned 3 mm below the quartz window of the cell. The Ag/AgCl reference electrode was connected by a Lugging probe of 0.5 mm inner diameter and positioned 2 mm from the iron surface. The counter electrode was a 10 mm diameter Pt ring disc. A peristaltic pump was used to allow circulation of the test solution to flow over the surface in order to cool the surface and thus prevent laser-induced heating of the surface. The Jobin-Yvon T64000 Raman spectrometer was used in single spectrograph mode with a holographic dispersive grating of 600 g/mm, giving a resolution of 2 cm^{-1}. The iron surface in the electrochemical

cell was analysed in back-scattering mode on the microscope stage of the Olympus confocal microscope attached to the spectrometer, with a long working distance 20x objective. The detector used was a liquid nitrogen cooled charge coupled device (CCD) detector. A 632.8 nm holographic notch filter was used to remove the reflected and Rayleigh-scattered light. Slit width was 200μm.

2.4. Scanning electron microscopy and energy dispersive X-ray investigations

The morphology of the formed layers on the iron surface after its immersion in 3.5% NaCl solutions in the presence of 1.0 mM TCDI for 72 h was investigated using a JEOL model JSM-6610LV (Japanese made) scanning electron microscope (SEM). The elemental analysis of the iron surface at the same condition was carried out using an energy dispersive X-ray (EDX) analyzer unit attached to the SEM machine.

3. RESULTS AND DISCUSSION

3.1. Open-circuit potential, scanning electron microscopy and energy dispersive X-ray investigations

The OCP experiments were carried out to report the effect of TCDI molecules on the behaviour of iron in test chloride solutions. The OCP curves for iron electrode in aerated 3.5% NaCl solution containing (1) 0.0, (2) 0.5, (3) 1.0, and (4) 2.0 mM TCDI are shown in Fig. 2.
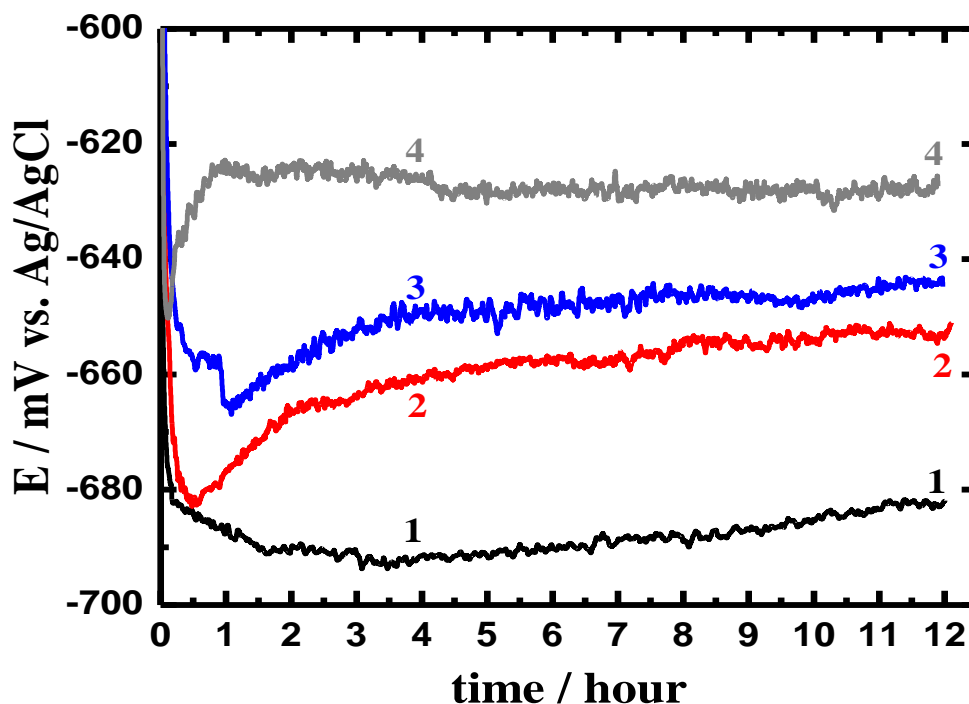
Figure 2. OCP curves for iron electrode in 3.5% NaCl solution containing (1) 0.0, (2) 0.5, (3) 1.0, and (4) 2.0 mM TCDI.

The potential of iron in chloride solution in absence of TCDI (curve 1) shifted toward the negative direction in the first few hours of iron immersion due to the dissolution of the surface by the aggressive chloride ions attack. This dissolution process helped in the formation of a layer of corrosion products, whose effect partially protected iron from further attack and could lead to the slight shift in the potential towards the less negative values with time.
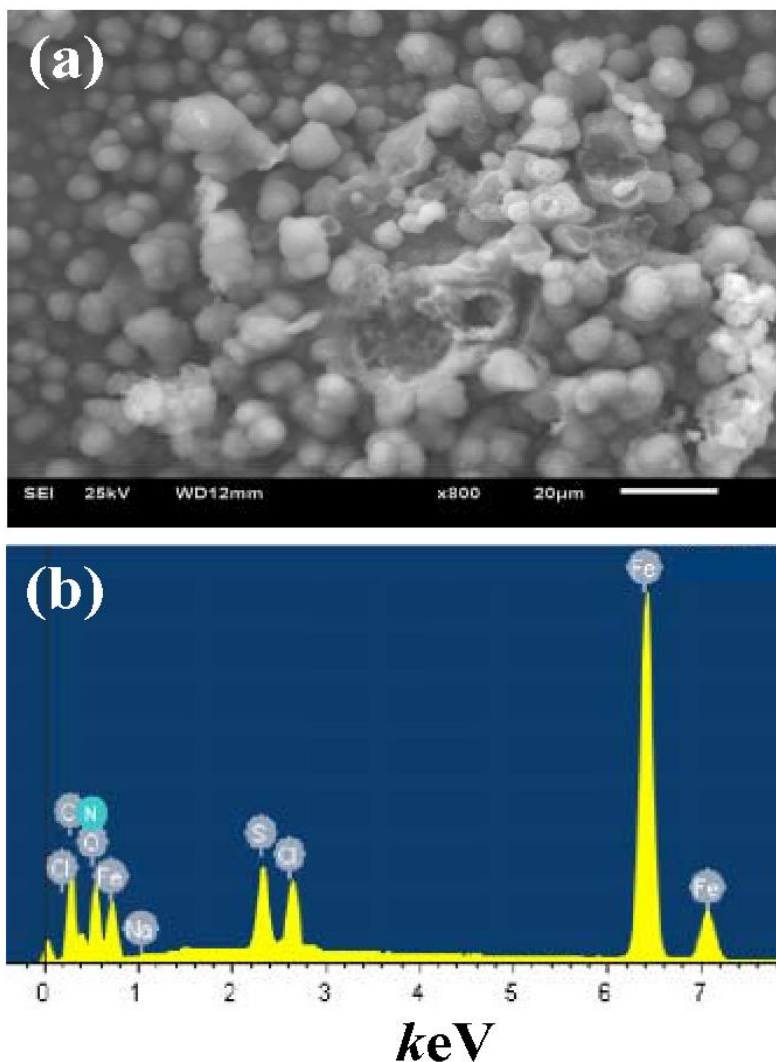
Figure 3. (a) SEM image obtained for iron surface after 72 h immersion in 3.5% NaCl + 1.0 mM
TCDI; and (b) EDX profile analysis of the iron surface shown in the micrograph.

In chloride solutions containing 0.5 mM (curve 2) and 1.0 mM (curve 3) TCDI, the potential showed rapid negative shift in the first few minutes, most probably due to the dissolution of the preformed oxide film that was formed on the iron surface in air before immersion into the test solution. The potential then shifted towards the positive values; this effect increased with increasing TCDI concentration. Furthermore, the presence of the highest concentration of TCDI, 2.0 mM as shown by curve 4, shifted the potential from the first moment of electrode immersion towards the positive direction and more positive shifts were recorded with increasing time. It is concluded from the

variation of the OCP of iron with time that the presence of TCDI and increase of its concentration shifted both the absolute and the steady state potential values to the more positive direction.

In order to understand the positive shifts of iron potential in the presence of TCDI, we carried out both SEM surface morphology and EDX investigations. The SEM micrograph obtained for the iron surface after 72 h immersion in 3.5% NaCl containing 1.0 mM TCDI is shown in Fig. 3a. The corresponding EDX profile analysis of the area shown in the SEM micrograph is shown in Fig. 3b. It is seen from the SEM micrograph that the TCDI molecules completely cover the metal surface. The weight and atomic percents of the elements found on the sample surface are shown on the EDX profile analysis. The detection of C, N, and S on the surface indicated that the TCDI molecules are indeed adsorbed on the surface. The presence of this high content of oxygen was perhaps due to the formation of an adherent oxide film due to the presence of oxygen in the solution. Moreover, the detection of low sodium and chlorine atoms gave an indication on the presence of some deposits of sodium chloride salt on the surface. Thus, the positive shifts in the OPC values, we have seen on Fig. 2, were due to the adsorption of TCDI molecules on the iron surface (*see also below, Raman data*). This indicates that increasing the concentration of TCDI increased the surface possibility to form a protective layer that got thicker with time and therefore precluded the corrosion of iron in chloride solutions.

3.2. Cyclic potentiodynamic polarization (CPP) measurements

Fig. 4 shows the CPP curves that were obtained for iron electrode after 1 h immersion in 3.5% NaCl containing (a) 0.0, (b) 0.50, (c) 1.0, and (d) 2.0 mM TCDI, respectively. These CPP experiments were carried out to study the effect of TCDI on the mitigation of pitting and uniform corrosion reactions on iron surface in 3.5% NaCl solutions. It is well known that the cathodic reaction for metals in aerated neutral solutions is the oxygen reduction according to,

$$2H_2O + O_2 + 4e^- = 4OH^- \tag{1}$$

This process consumes the electrons that are released during the oxidation reaction, where the corrosion of iron can undergo two different transformations as follows [1],

$$Fe = Fe^{2+} + 2e^- \tag{2}$$

$$Fe^{2+} = Fe^{3+} + e^- \tag{3}$$

Nevertheless, in practice the second transformation, eq. (3), will not occur. While the dissolution of iron in concentrated NaCl solutions into ferrous cations can be explained according to Darwish et al. [19],

$$Fe + H_2O = Fe(OH)_{ads} + H^+ \tag{4}$$

$$Fe + Cl^- = Fe(Cl^-)_{ads} \tag{5}$$

$$Fe(OH)_{ads} + Fe(Cl^-)_{ads} = Fe + FeOH^+ + (Cl^-) + 2e^- \tag{6}$$

$$FeOH^+ + H^+ = Fe^{2+}_{aq} + H_2O \tag{7}$$

In addition, the hydroxide ions resulting from eq. (1) will react with Fe^{2+} to form a deposit of $Fe(OH)_2$,

$$Fe + \tfrac{1}{2} O_2 + H_2O = Fe(OH)_2 \tag{8}$$

If there is an excess of oxygen presented, the formed ferrous hydroxide transforms to the final corrosion product that is called magnetite (Fe_3O_4) according to the following reaction,

$$3Fe(OH)_2 + \tfrac{1}{2} O_2 = Fe_3O_4 + 3H_2O \tag{9}$$
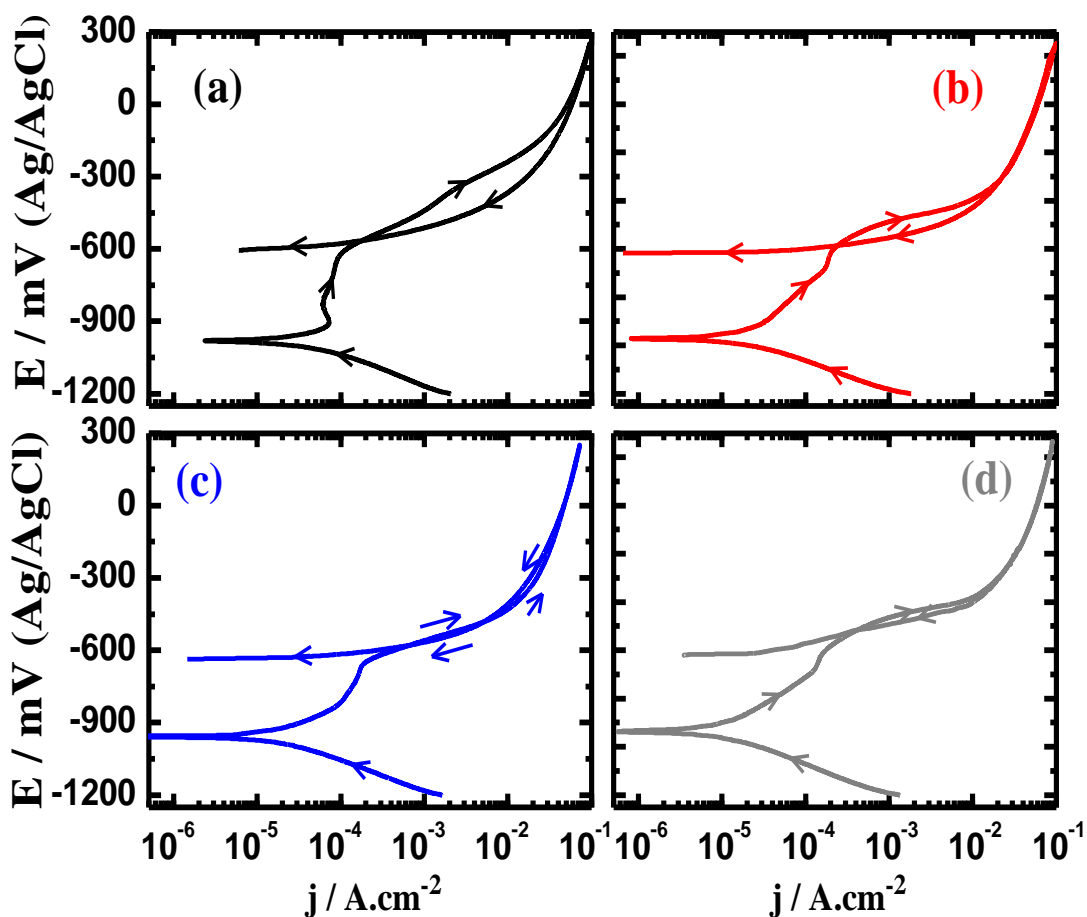
Figure 4. Cyclic potentiodynamic polarization curves for iron electrode after its immersion for 1 h in 3.5% NaCl solution containing (a) 0.0, (b) 0.5, (c) 1.0, and (d) 2.0 mM TCDI.

The anodic reactions on iron surface after 1 h and 24 h in chloride solutions at the same condition were reported in the previous study [1]. In brief, the polarization curve for iron (Fig. 4a) shows a short active-passive region due to the dissolution of iron, as shown by eqs 4, 5, 6, and 7, and the formation of corrosion products and/or oxide layers, as indicated by reaction (8) and reaction (9), respectively. At more positive potential values, the formed passive film dissolved due to the rapid increase of current of iron. Scanning the potential in the backward direction showed higher currents than those of the forward ones. According to Rosen and Silverman [20] increasing the back scan current values compared to the forward ones lead to the appearance of a hysteresis loop on the cyclic polarization curve, which confirms the occurrence of pitting corrosion [20]. The severity of pitting corrosion is directly proportional to the increase of back scan current values and the size of the hysteresis loop. The values of the corrosion current (j_{Corr}), corrosion potential (E_{Corr}), anodic (β_a) and cathodic (β_c) Tafel slopes, polarization resistance (R_P), corrosion rate (K_{Corr}), and percentage of the inhibition efficiency (*IE%*) obtained from Fig. 4 are listed in Table 1. The values of these parameters were obtained as reported in the previous studies [1, 21–32].

Table 1. Corrosion parameters obtained from cyclic potentiodynamic polarization curves shown in Fig. 4 for iron after its immersion for 1 h in 3.5% NaCl solutions without and with TCDI.

Solution	Parameter						
	E_{Corr} / mV	j_{Corr} / $\mu A\ cm^{-2}$	β_c / mV dec^{-1}	β_a / mV dec^{-1}	R_p / $\Omega\ cm^2$	R_{Corr} / mmy^{-1}	*IE* / %
NaCl alone	-995	15	120	105	1620	0.175	—
+ 0.5 mM TCDI	-980	9	122	115	2860	0.105	40
+ 1.0 mM TCDI	-955	6.2	125	125	4380	0.072	58.7
+ 2.0 mM TCDI	-935	2.8	130	135	10280	0.033	81.3

The presence of TCDI and the increase of its concentration (Fig. 4b, c, and d) significantly decreased the values of j_{Corr} and in a direct proportionality the K_{Corr} as well as positively shifted E_{Corr} to the less negative values, while increased the values of R_P and *IE%*. The decrease of j_{Corr} and K_{Corr} with the high increase of R_P and *IE%* values on the addition of TCDI and up on the increase of its concentration was due to the decrease of iron uniform corrosion. On the other hand, the decrease then the disappearance of the hysteresis loop area on the polarization curves indicated on the increase of iron resistance against pitting corrosion, especially at high TCDI concentration, 2.0 mM [20]. It is worth to mention also that the anodic branch of the polarization curve in case of 3.5% NaCl in the absence of TCDI molecules showed large passive region due to the formation of iron oxides and chlorides as represented by eqs (1–9). This passive region decreased in the presence of TCDI molecules and further with the increase of its concentration due to the fact that the adsorption of TCDI molecules on the iron surface inhibits the dissolution of iron through decreasing both the anodic and cathodic reactions and thus decreased the formation of these iron oxide and chloride compounds.

3.3. Potentiostatic current-time measurements

In order to confirm whether TCDI decreases the pitting and uniform corrosion reactions on iron surface at less negative potential value than the OCP, potentiostatic current-time experiments were carried out. Fig. 5 shows the potentiostatic current-time curves obtained at –500 mV vs. Ag/AgCl for iron electrode after its immersion for 1 h in 3.5% NaCl solution containing (1) 0.0, (2) 0.5, (3) 1.0, and (4) 2.0 mM TCDI. The initial currents started low and increased with increasing time for iron in chloride solution alone (curve 1). This is due to the rapid dissolution of iron as represented by Eq. (2) and the formation of iron hydroxide, which transfers to magnetite as shown by Eq. (8) and Eq. (9). The iron then recorded the highest absolute currents with increasing time because of its dissolution under the high applied potential and the aggressiveness action of the chloride ions and as shown by eqs (4–7). The presence of high Cl^- concentration with the ferrous cations in the solution would allow the formation of $FeCl_2$ and $FeCl_3$ as follows,

$$Fe\ (s) + 2Cl^-\ (aq) = FeCl_2\ (s) + 2e^- \tag{10}$$

$$FeCl_2\ (s) + Cl^-\ (aq) = FeCl_3\ (s) + e^- \tag{11}$$
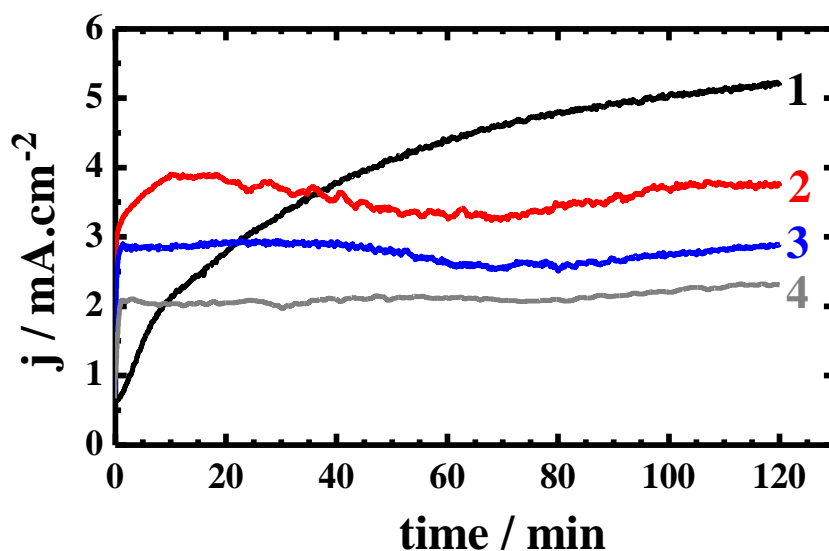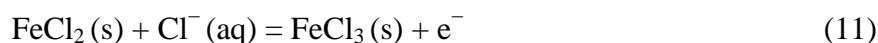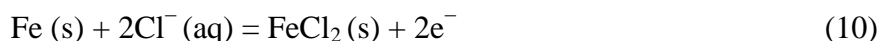
Figure 5. Potentiostatic current-time curves obtained at -500 mV vs. Ag/AgCl for iron electrode after its immersion for 1 h in 3.5% NaCl solution containing (1) 0.0, (2) 0.5, (3) 1.0, and (4) 2.0 mM TCDI.

As a result of the applied potential and concentration gradients and as reported in our previous work [1], the $FeCl_2$ and $FeCl_3$ species at the interface diffused through the porous film and the diffusion boundary layer then carried away to the bulk solution by convection. This could lead to the continuous dissolution of iron as well as the occurrence of pitting corrosion of iron as indicated by the gradual increase of iron current with time. This was not the case for iron in the presence of TCDI

molecules. Where, at 0.50 mM TCDI (Fig. 5, curve 2) the current slightly increased in the first 10 min, after which the current decreased gradually. This initial increase of current was due to the sudden change of the potential of iron from OCP to the more active value, −500 mV, while the gradual decrease of current with time resulted from the increased surface resistance due to the adsorption of TCDI molecules. The addition of 1.0 mM TCDI as seen from Fig. 5, curve 3, showed similar current-time behaviour but with large decreases in the absolute current. Increasing the concentration of TCDI further to 2.0 mM led to further decreases in the absolute currents with time. This change of current with time indicated that the iron electrode suffered both pitting and uniform corrosions in the reported concentration of chloride solution and the presence of TCDI and increase of its concentration mitigated the pitting and uniform corrosion reactions. This was achieved by the adsorption of TCDI molecules (*see below, Raman data*), to cover up iron, which in turn isolated the surface from being exposed to the harsh chloride solution.

3.4. In-situ Raman spectroscopy investigations

In-situ Raman spectroscopy investigations were carried out to confirm whether the TCDI molecules are indeed adsorbed as well as the molecular structure of the film formed on iron surface in chloride solutions at different potentials. The in-situ Raman spectra obtained on the iron surface after its immersion in 3.5% NaCl solution containing 1.0 mM TCDI for (a) 1 h at OCP and (b) after its immersion in the same solution for 1 h before stepping the potential to −500 mV for 2 h are shown in Fig. 6a and Fig. 6b, respectively.
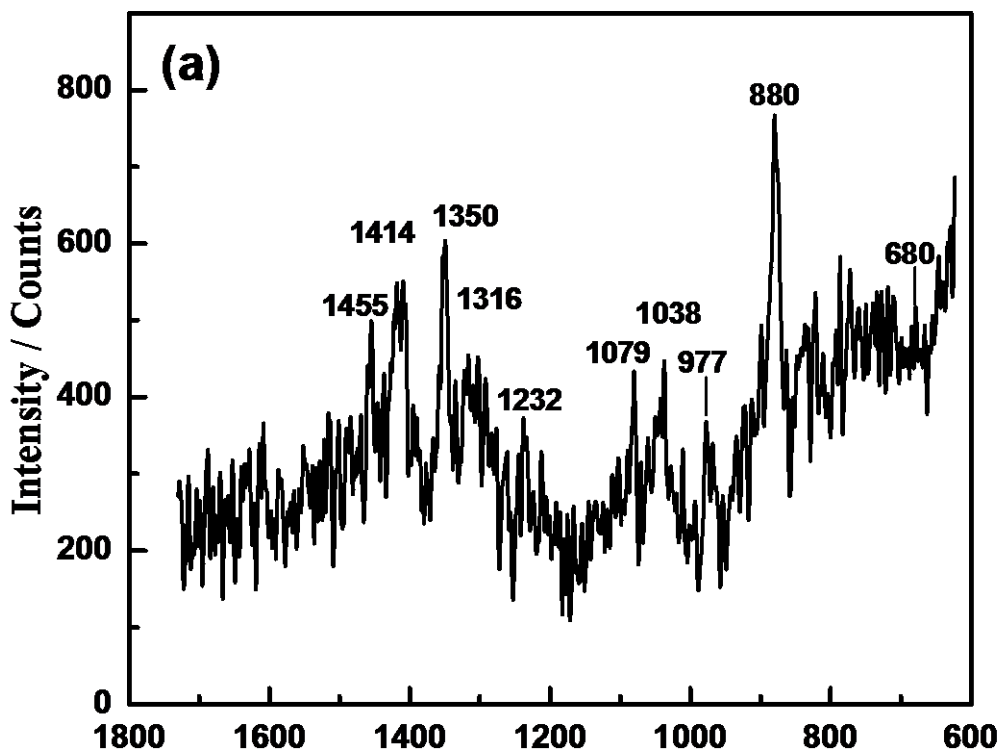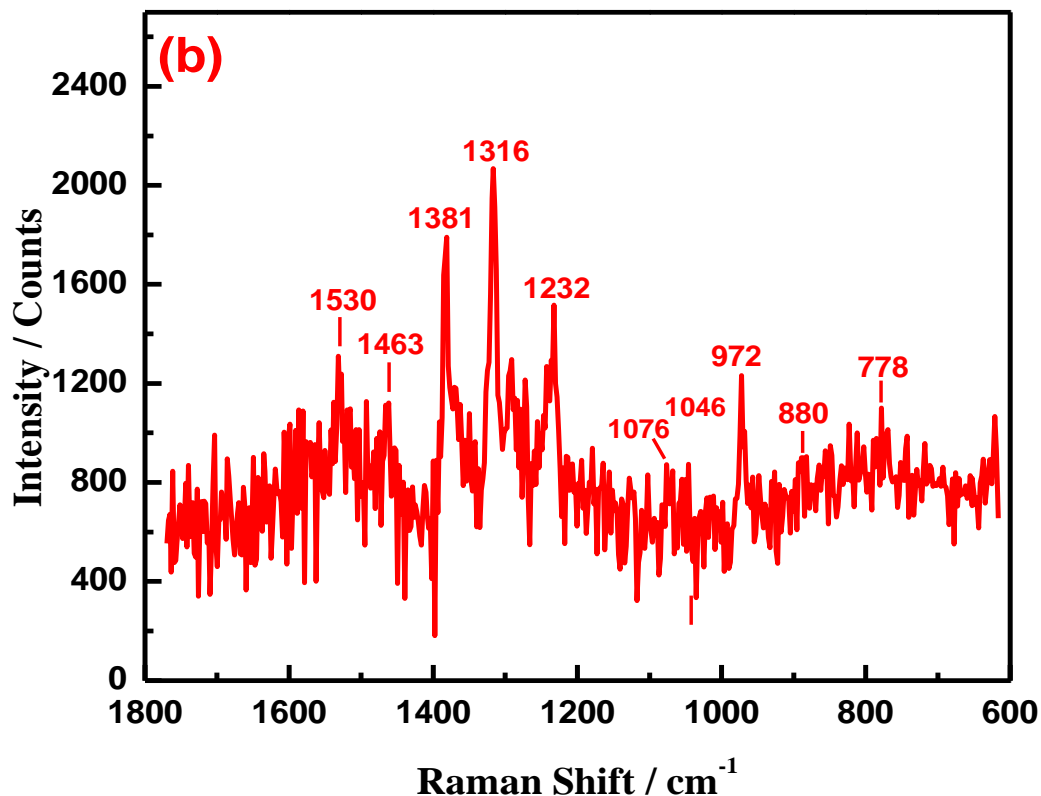
Figure 6. In-situ Raman spectra obtained on the iron surface that was immersed in 3.5% NaCl solution containing 1.0 mM TCDI; (a) at free open-circuit potential after 1 h immersion, and (b) after 1 h immersion followed by stepping the potential at -500 mV vs. Ag/AgCl for 2 h.

The spectrum of Fig. 6a shows several bands at 680, 880, 977, 1038, 1079, 1232, 1316, 1350, 1414, and 1455 cm^{-1}. The weak band at 680 cm^{-1} is related to a very thin iron oxide film, most probably magnetite (Fe_3O_4) [33]; the strong bands at 880 cm^{-1}, 1038 cm^{-1}, 1079 cm^{-1}, 1232 cm^{-1}, and 1414 cm^{-1} were also appeared on the iron surface at similar conditions in the presence of 3-amino-5-mercapto-1,2,4-triazole and were due to the ring breathing and in-plane ring-stretching vibrations (9); 1232 cm^{-1} due to C=C vibrations of the imidazole rings, 1316 and 1414 cm^{-1} due to the interaction of the organic compound through away or another with the iron surface; 1350 cm^{-1} ring stretching due to N–H deformation [1, 34–36).The majority of the Raman mode assignments thus prove the presence of TCDI or its complex with iron in the formed film through its adsorption then polymerization onto the surface. The Raman spectrum obtained for the iron surface after its immersion in 3.5% NaCl + 1.0 mM TCDI for 1 h before applying -500 mV for 2 h, Fig. 6b, showed almost similar bands and confirmed the existing of TCDI molecules on the iron surface. This indicates that the decrease of the absolute current and the disappearance of pitting corrosion we have seen on curve 3 of Fig. 5 were due to the adsorption of TCDI or its complex onto the electrode surface.

In order to further confirm the adsorption of TCDI molecules, in-situ Raman spectroscopy was carried out on the iron surface after its immersion in 3.5% NaCl + 1.0 mM TCDI for 20 min at –1.2, –0.9, –0.7, –0.55, –0.4 and –0.3 V, respectively and the spectra are shown in Fig. 7. The majority of the Raman modes observed are characteristic of the presence of TCDI or its complex with iron in the

film formed at –1.2, –0.9, –0.7, and –0.55 V. The Raman spectra show almost similar bands like we have seen in Fig. 6, these bands namely are 880, 1038, 1086, 1146, 1234, 1311, 1352, and 1411 cm^{-1}. The Raman results at these potential values thus emphasis the assumption that TCDI molecules are strongly adsorbed onto the iron surface and therefore, strongly supporting the model invoking the blocking its active sites and preventing it from being corroded easily.
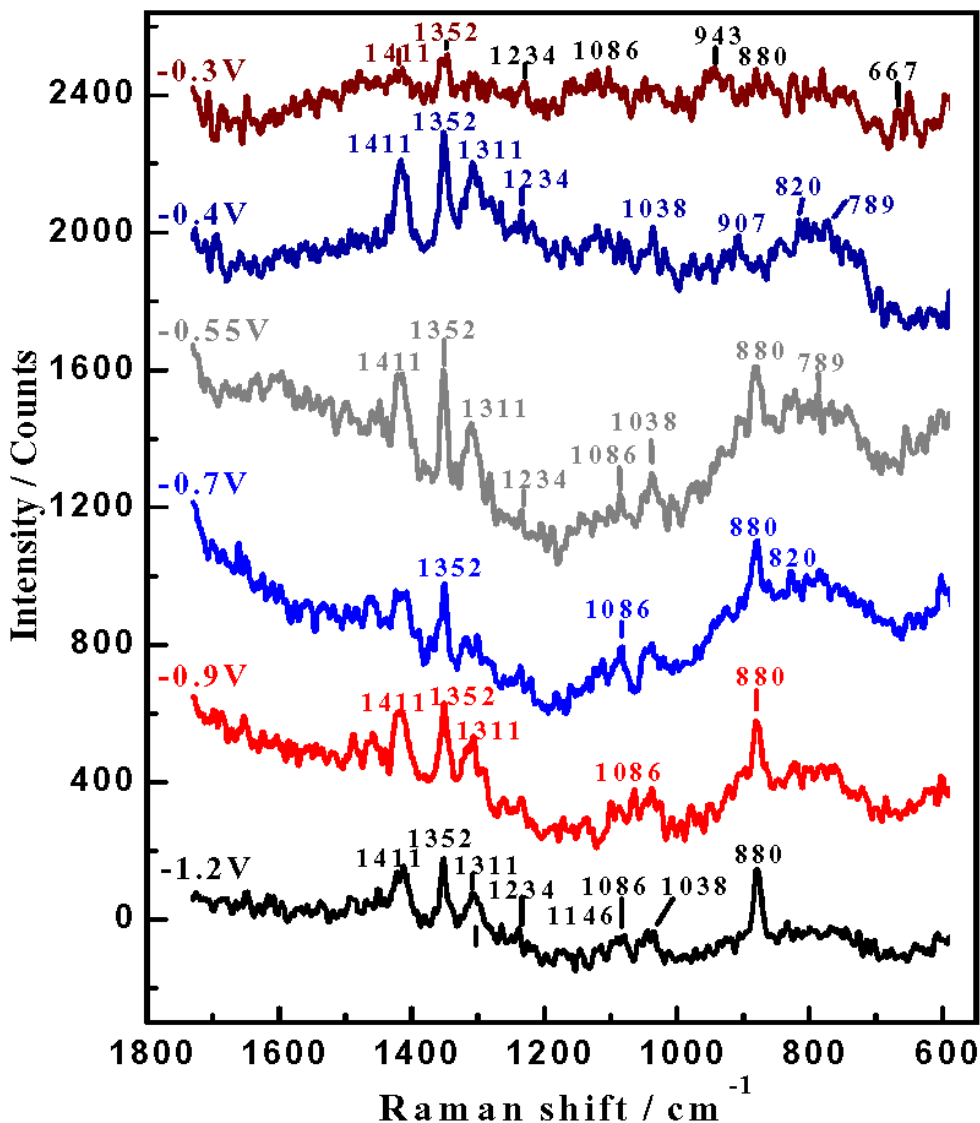
Figure 7. In-situ Raman spectra obtained for iron at different potential values after 20 min of the electrode immersion in 3.5% NaCl solution containing 1.0 mM TCDI.

3.5. Electrochemical impedance spectroscopy (EIS) measurements

The Nyquist (a), Bode (b) and phase angle (c) plots for iron electrode after 1 h immersion in 3.5% NaCl solution containing (1) 0.0, (2) 0.5, (3) 1.0, and (4) 2.0 mM TCDI, respectively are shown

in Fig. 8. Both the Nyquist and Bode plots are included in Fig. 8 for better understanding of the system under investigation as well as to determine kinetic parameters for electron transfer reactions at the iron/electrolyte interface.

The impedance spectrum for the Nyquist plots were analysed by fitting to the equivalent circuit model shown in Fig. 9 and has been previously used to model the iron/neutral chloride interface [1, 15]. The parameters obtained by fitting the equivalent circuit and the values of the calculated percentage of the inhibition efficiency, *IE%,* are listed in Table 2. These parameters are defined as follows; R_S represents the solution resistance, Q the constant phase elements (CPEs), *and* R_P the polarization resistance and can be referred also as the charge transfer resistance (R_{ct}).

Table 2. EIS parameters obtained by fitting the Nyquist plots shown in Fig. 8a and the equivalent circuit shown in Fig. 9 for iron in chloride solutions in absence and presence of TCDI.

Parameter Solution	R_s / Ω cm^2	Q (CPEs) $Y_Q / \mu F$ cm^{-2}	n	R_p / Ω cm^2	IE / %
NaCl alone	6.67	7.65	0.77	640	−
+ 0.5 mM TCDI	8.00	6.04	0.80	1120	42.9
+ 1.0 mM TCDI	10.1	4.86	0.80	1960	67.3
+ 2.0 mM TCDI	12.7	4.11	0.80	3370	81.0

It is seen from Fig. 8a that the semicircles at high frequencies are generally associated with the relaxation of electrical double layer capacitors and the diameters of the high frequency semicircles can be considered as the charge transfer resistance [1]. It is also seen from Table 2 that the presence of 0.5 mM TCDI enhanced the values of R_S and R_P, while reduced the value of Y_Q. The constant phase element (CPE) can be defined in impedance representation as follows [15]:

$$Z(CPE) = (Y_0^{-1})\,(j\omega)^{-n} \qquad\qquad (12)$$

Where, Y_0 is the CPE constant, ω is the angular frequency (in rad s^{-1}), $j^2 = -1$ is the imaginary number and n is the CPE exponent. Depending on the value of n, CPE can represent resistance (Z(CPE) = R, n = 0), capacitance (Z(CPE) = C, n = 1), inductance (Z(CPE) = L, n = −1) or Warburg impedance for (n = 0.5). In this work the value of n was almost 0.8 for all solutions, which means that the constant phase elements represent a capacitor but not pure due to the heterogeneity or the presence of little porosities in the formed layer on the iron surface. Hence, the CPE is substituted for the capacitor to fit the semicircle more exactly.
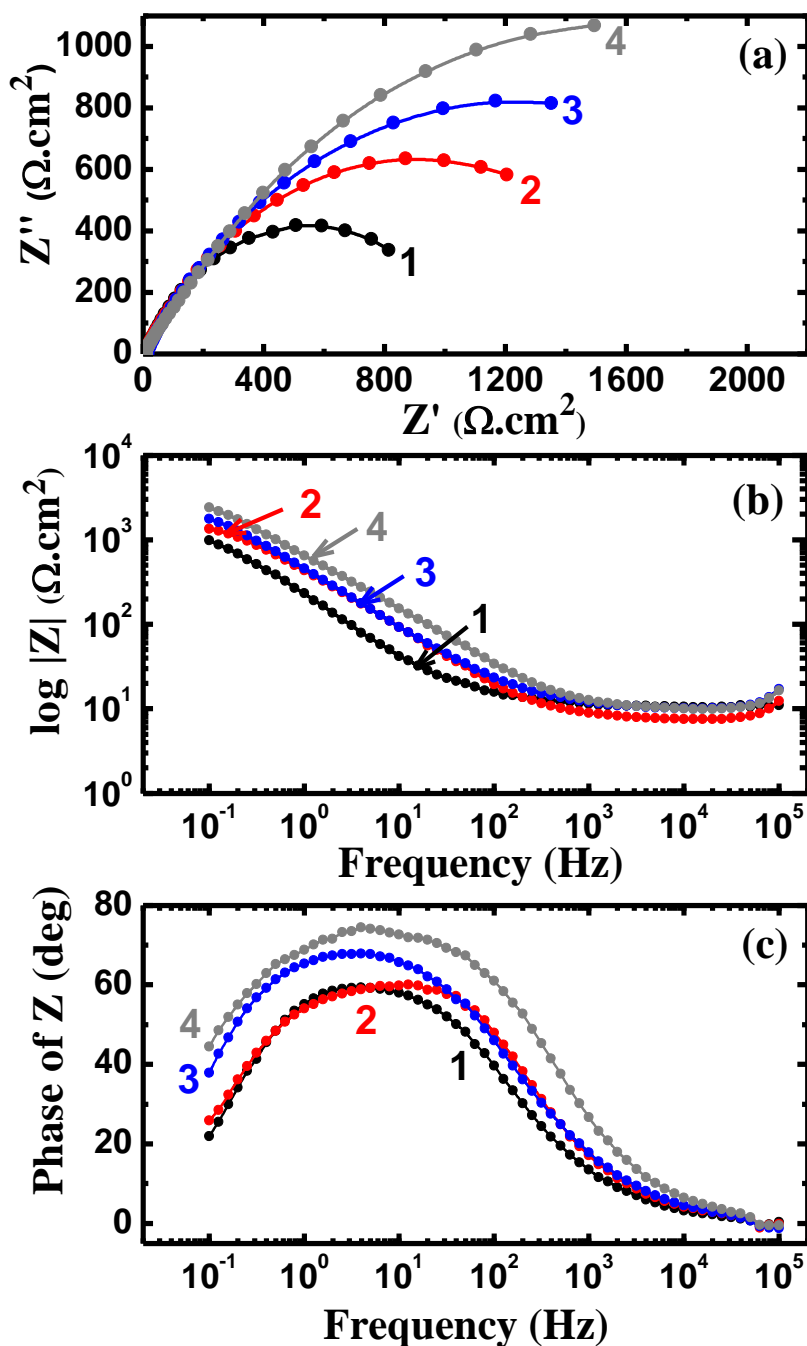
Figure 8. Nyquist (a), Bode (b) and phase angle (c) plots for iron electrode after 1 h immersion in 3.5% NaCl solution containing (1) 0.0, (2) 0.5, (3) 1.0, and (4) 2.0 mM TCDI.

The CPEs decrease in the presence of TCDI and upon increasing its concentration in the solution is due to the reduction of the capacitive effects by the charged iron surfaces. The values of *IE*% values of TCDI for the iron electrode were calculated from the charge transfer resistance as previously reported [1]. This effect was increased with raising the concentration of TCDI to 1.0 mM and further with 2.0 mM. There is also an agreement between the EIS and polarization data, which is well defined by the comparable and increased values of *IE*% that were calculated from the parameters of both techniques with increasing the organic compound. The ability of TCDI as a good corrosion

inhibitor was also proven by the increase of the impedance of the interface (Fig. 8b), especially at the low frequency range, which indicates the more passivated is the iron surface with the increase of TCDI concentration.
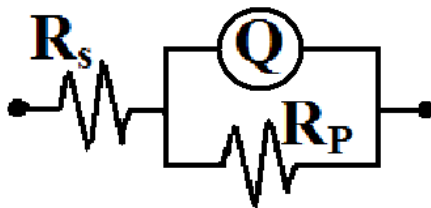
Figure 9. Equivalent circuit model used to fit the EIS experimental data presented in Fig. 8a. See text for symbols used in the circuit.

The maximum phase angle, Fig. 8c, also increases and reveals the powerful inhibition effectiveness of TCDI, which increases significantly with the increase of its concentration [21-23].

4. CONCLUSIONS

The corrosion and corrosion inhibition of pure iron in aerated 3.5% sodium chloride solutions by 1,1'-thiocarbonyldiimidazole (TCDI) has been investigated using a variety of electrochemical methods, SEM/EDX, and in-situ Raman spectroscopy measurements. Severe uniform and pitting corrosion reactions were recognized on iron in the test solution of aerated 3.5% NaCl. These reactions were minimized in the presence of TCDI molecules and up on the increase of its concentration as revealed by electrochemical measurements. The decrease of severity of these reactions was attributed to the adsorption of TCDI molecules, which were detected on the iron surface after it was immersed in chloride containing TCDI solutions as confirmed by SEM/EDX as well as in-situ Raman spectroscopy investigations. The results are collectively in good agreement indicating that TCDI molecules were able to eliminate the uniform and pitting corrosion reactions on iron surface in 3.5% NaCl solutions and this ability increases with increasing TCDI concentration.

References

1. E.M. Sherif, R.M. Erasmus, J.D. Comins, *Electrochim. Acta,* 55 (2010) 3657–3663.
2. H. Amar, A. Tounsi, A. Makayssi, A. Derja, J. Benzakour, A. Outzourhit, *Corros. Sci.,* 49 (2007) 2936.
3. A.N. Abdelhadi1, G.Y. Abbasi, F.M. Saeed, *Int. J. Electrochem. Sci.,* 5 (2010) 1665.

4. N.A. Al-Mobarak, *Int. J. Electrochem. Sci.,* 3 (2008) 666.
5. S. Agnesia Kanimozhi, S. Rajendran, *Int. J. Electrochem. Sci.,* 4 (2009) 353.
6. V.F. Ekpo1, P.C. Okafor, U.J. Ekpe, E.E. Ebenso, *Int. J. Electrochem. Sci.,* 6 (2011) 1045.
7. E.F. Diaz, J.G. Gonzalez-Rodriguez, R. Sandoval-Jabalera, S. Serna, B. Campillo, M.A. Neri-Flores, C. GaonaTiburcio, A. Martinez-Villafañe, *Int. J. Electrochem. Sci.,* 6 (2011) 1479.
8. E.M. Sherif, *Inter. J. Electrochem. Sci.,* 5 (2010) 1821.
9. E.M. Sherif, S.-M. Park, *J. Electrochem. Soc.,* 152 (2005) B205.
10. E.M. Sherif, S.-M. Park, *Electrochem. Acta,* 51(2006) 1313.
11. E.E. Ebenso, I.B. Obot, L.C. Murulana, *Inter. J. Electrochem. Sci.,* 5 (2010) 1574.
12. M. Lebrini, F. Robert, C. Roos, *Int. J. Electrochem. Sci.,* 6 (2011) 847.
13. P.C. Okafor, E.E. Ebenso, U.J. Ekpe, *Int. J. Electrochem. Sci.,* 5 (2010) 978.
14. M. Scendo, M. Hepel, *J. Electroanal. Chem.,* 613 (2008) 35.
15. Z. Zhang, S. Chen, Y. Li, S. Li, L. Wang, *Corros. Sci.,* 51 (2009) 291.
16. X.R. Ye, X.O. Xin, J.J. Zhu, Z.L. Xue, *Appl. Surf. Sci.,* 135 (1998) 307.
17. F. Farelas, A. Ramirez, *Inter. J. Electrochem. Sci.,* 5 (2010) 797.
18. I. Lukovits, E. Kalman, F. Zucchi, *Corrosion*, 57 (2001) 3.
19. N. A. Darwish, F. Hilbert, W.J. Lorenz, H. Rosswag, *Electrochim. Acta,* 18 (1973) 421.
20. E.M. Rosen, D. C. Silverman, *Corrosion,* 48 (1992) 734.
21. E.M. Sherif, R.M. Erasmus, J.D. Comins, *J. Colloid Interface Sci.,* 311 (2007) 144.
22. E.M. Sherif, R.M. Erasmus, J.D. Comins, *J. Colloid Interface Sci.*, 306 (2007) 96.
23. E.M. Sherif, R.M. Erasmus, J.D. Comins, *J. Colloid Interface Sci.*, 309 (2007) 470.
24. E.M. Sherif, R.M. Erasmus, J.D. Comins, *Corros. Sci.,* 50 (2008) 3439.
25. E.M. Sherif, A.A. Almajid, *J. Appl. Electrochem.*, 40 (2010) 1555.
26. E.M. Sherif, *J. Appl. Surf. Sci.,* 252 (2006) 8615.
27. E.M. Sherif, *J. Mater. Eng. Perform.,* 19 (2010) 873.
28. E.M. Sherif, A.Y. Ahmed, *Synthesis and Reactivity in Inorganic, Metal-Organic, and Nano-Metal Chemistry,* 40 (2010) 365.
29. E.M. Sherif, A.A. Almajid, F.H. Latif, H. Junaedi, *Int. J. Electrochem. Sci.,* 6 (2011) 1085.
30. E.M. Sherif, J.H. Potgieter, J.D. Comins, L. Cornish, P.A. Olubambi, C.N. Machio, *J. Appl. Electrochem.,* 39 (2009) 1385.
31. E.M. Sherif, J.H. Potgieter, J.D. Comins, L. Cornish, P.A. Olubambi, C.N. Machio, *Corros. Sci.,* 51 (2009) 1364.
32. E.M. Sherif, A.A. Almajid, *Int. J. Electrochem. Sci.,* 6 (2011) 2131.
33. L.J. Simpson, C.A. Melenders, *Electrochim. Acta,* 41 (1996) 1727.
34. N.H.T. Le, M.C. Bernard, B. Garcia-Renaud, C. Deslouis, *Synth. Met.,* 140 (2004) 287.
35. P.M.L. Bonin, W. Jędral, M.S. Odziemkowski, R.W. Gillham, *Corros. Sci.,* 42 (2000) 1921.
36. I. Harada, Y. Furukawa, F. Ueda, *Synth. Met.,* 29 (1989) 303.